Theor Chem Acc (2003) 110: 360–366
DOI 10.1007/s00214-003-0488-5

Theoretical
Chemistry Accounts

Regular article

Rayleigh and Raman light scattering in hydrogen-bonded acetonitrile–water

Eduardo Rissi, Eudes E. Fileti, Sylvio Canuto

Instituto de Física, Universidade de São Paulo, CP 66318, 05315-970 São Paulo, SP, Brazil

Received: 3 September 2002 / Accepted: 30 April 2003 / Published online: 1 December 2003

Abstract. The structure, vibrational frequencies, light scattering activities and binding energies of $CH_3CN\cdots H_2O$ are obtained from ab initio methods. The hydrogen $N\cdots H$ bond distance is calculated as 2.06 Å, the dipole moment as 5.77 D and our best estimate for the binding energy is 3.5 kcal mol^{-1} (14.7 kJ mol^{-1}), after correcting for zero-point vibrations. The calculated average dipole polarizability is 39.67 au and the anisotropy is fairly large, corresponding to 21.78 au. The changes in intramolecular vibrational frequencies are analyzed. The scattering activities and depolarization of the Rayleigh and Raman light scattered are calculated. In the Raman case the depolarization due to the intense NC stretching vibration is increased by 20% after the hydrogen bond. For the OH symmetric stretch of water there is a large redshift of 75 cm^{-1} and a great intensification of the Raman scattering activity by a factor of 2 and a considerable increase of the depolarization by a factor of nearly 4.

Keywords: Hydrogen bond – Acetonitrile – Infrared shift – Dipole polarizabilities – Light scattering

Introduction

The study of the acetonitrile–water (CH_3CN–H_2O) system is very important for understanding binary mixtures [1] leading to powerful solvents with applications in chemistry and environment studies [2]. Acetonitrile–water ionic clusters play an important role in the terrestrial atmosphere [3] and CH_3CN is of great interest in astrophysics [4, 5, 6, 7]. A more detailed understanding of the acetonitrile–water interaction should consider the important hydrogen-bond interaction. With the development of laser vaporization and jet cooling techniques the field of cluster physical chemistry has seen great advances [8, 9, 10] and hydrogen-bonded clusters have been produced [11, 12, 13]. Indeed, hydrogen-bonded $CH_3CN\cdots H_2O$ clusters have been produced in supersonic beam experiments [14, 15]. In addition, the hydrogen bond is a topic of continuing interest in physics, chemistry and biology [11, 16, 17]. The hydrogen-bonded system $CH_3CN\cdots H_2O$ has been of interest for many years and has been studied theoretically (at the Hartree–Fock, HF, level) [18], experimentally [14, 15] and its vibrational spectrum has been studied in inert matrices [19]. In a theoretical and experimental work, Desfrançois et al. [14] suggested two stable structures (Fig. 1), although they just observed the apparently stablest one (Fig. 1a), with a calculated total dipole moment of 5.5 D. They suggested [14, 15] an isomer with a total dipole moment of 2.6 D, possibly being a second stable geometry. The identification of cluster structures is difficult to achieve directly and usually approaches rely on the comparison between theoretical and experimental spectral shifts. For closed-shell polar molecules a suitable procedure [14, 15] compares theoretical and experimental dipole moments. Hydrogen bonds can, however, be studied with a great variety of techniques and spectral shifts in the IR region is perhaps the most widely used technique. Despite its importance, accurate theoretical calculations of the acetonitrile–water system are still missing. In this work we use ab initio calculations to obtain the structure and spectrum of the $CH_3CN\cdots H_2O$ complex. To contribute to the understanding of the experimental spectral changes we calculate the IR shifts upon complexation and the dipole moments of the complex and the separate moieties. The change in the depolarization ratio for both elastic (Rayleigh) and inelastic (Raman) light scattering is also of great interest. Hence, we calculate the dipole

From the Proceedings of the 28th Congreso de Químicos Teóricos de Expresión Latina (QUITEL 2002)

Correspondence to: S. Canuto
e-mail: canuto@if.usp.br

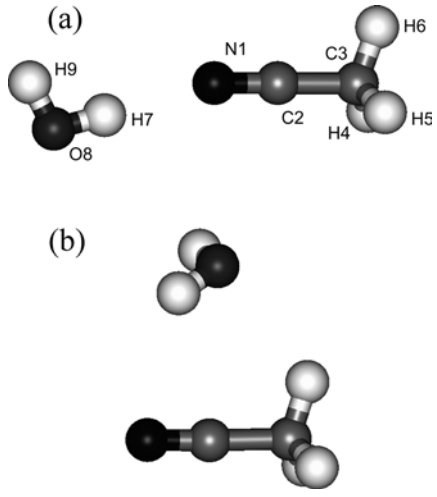

Fig. 1. Geometrical structures of the acetonitrile–water hydrogen-bonded complex

polarizability tensor, the polarizability derivatives with respect to the vibrational modes and the Rayleigh and Raman scattering activities and depolarizations of $CH_3CN\cdots H_2O$ and compare the results with those obtained for the two isolated species. We also present an accurate estimate for the binding energy, using high-level ab initio calculations obtained at the coupled-cluster level with large basis sets and including corrections for basis set superposition and zero-point energy vibrations.

Methods

Full geometry optimization was performed using four theoretical models: MP2/6-311++G(d,p), MP2/aug-cc-pVDZ, B3LYP/6-311++G(d,p) and B3P86/6-311++G(d,p). As usual, MP2 stands for second-order perturbation in the Møller–Plesset partitioning. The density functional theory (DFT) calculations use two of the most common gradient-corrected functionals: Becke's three-parameter hybrid functional combining the Lee–Yang–Parr correlation term [20, 21], namely B3LYP, and Becke's three-parameter hybrid functional with the Perdew correlation term [22], B3P86. These methods were used with the 6-311++G(d,p) and the aug-cc-pVDZ basis sets [23]. In all cases the rotational constants and dipole moments were calculated in the equilibrium geometries. These are the relevant parameters for characterization of geometrical structures using rotational spectroscopy. The calculation of theIR spectrum was performed for isolated water, CH_3CN and $CH_3CN\cdots H_2O$. Shifts in the vibrational frequencies upon complexation resulting in the formation of $CH_3CN\cdots H_2O$ were also calculated. Particular attention is devoted to the most intense transitions and the CN and OH stretching vibrations. Additionally, the hydrogen binding energies for the complex were calculated and the contribution of the electron correlation effect was systematically analyzed. In these geometries we performed single-point calculations with many-body perturbation theory of second, third and fourth order and with quantum-chemical coupled-cluster theory with single and double excitations (CCSD) and single, double and partial triple excitations, CCSD(T) [24]. This allows a systematic analysis of the electron correlation contribution to the binding energy. Full counterpoise correction for the basis set superposition error (BSSE), as proposed by Boys and Bernardi [25], was taken into account for all the calculated binding energies. The depolarization ratios for Rayleigh and Raman scattering were calculated after obtaining the dipole polarizabilities (average and anisotropic) and their derivatives at the correlated level using the consistent MP2/aug-cc-pVDZ level. All the calculations were performed with the Gaussian 98 program [26].

Results

Geometries, rotational constants and dipole moments

The structures obtained in this work are shown in Fig. 1. The structure in Fig. 1b has been obtained before at the HF level [18] and has been considered in experimental situations [15]. However the structures were found here to be unstable at higher levels of calculation. Indeed, using small basis sets [6-31G(d,p)] it was possible to get a stable minimum at the uncorrelated HF level and correlated levels such as MP2, B3LYP and B3P86. However, improvement of the theoretical model led invariably to an unbound structure. Using the MP2/6-31G(d,p) model we find that the complex is bound with an O–C(N) distance of 3.056 Å and a binding energy of only 2 kcal mol^{-1} (after correcting for basis set superposition error and zero-point vibration corrections). The calculated total dipole moment for this complex is 2.43 D. The corresponding dipole moments calculated at the B3LYP/6-31G(d,p) and B3P86/6-31G(d,p) levels are 2.58 and 2.62 D. These are in good agreement with the value of 2.6 D inferred using theoretical multipolar development [14]. However, as this structure is found to be unstable after improvement of the theoretical model, we give it no further consideration. The structure in Fig. 1a is found to be a true stable minimum using all the theoretical levels considered here. To assess the results more critically the four different calculations for the geometry, rotational constants and dipole moments of the acetonitrile–water complex (Fig. 1a) and its moieties are shown in Table 1. Experimental values for the geometry of gaseous CH_3CN give the NC distance as 1.59 Å [27]. The DFT results give NC distances in good agreement with experiment. These are shorter than those obtained with MP2 and this is consistent with its triple-bond nature. However, all the theoretical methods agree that this NC distance decreases by 0.002 Å after hydrogen binding with water. In contrast, in water, as expected, the OH distance involved in the binding increases by 0.005–0.008 Å, depending on the theoretical model. The least increase is obtained with MP2/6-311++G(d,p) and the largest increase with B3P86/6-311++G(d,p). A consequence of the decrease in the NC distance will be a blueshift in the NC stretching vibration frequency as shown later.

After complexation the $CH_3CN\cdots H_2O$ system still behaves as a nearly prolate rotor and the corresponding rotational constants are also given in Table 1. In polar clusters prepared by supersonic beam experiments, dipole moments are required to deduce structural information [15]; so the calculated dipole moments are also given in Table 1. The experimental result [28] of 1.86 D for the dipole moment of gas-phase water is well reproduced only in the MP2/aug-cc-pVDZ model.

Table 1. Optimized geometry of the $CH_3CN\cdots H_2O$ complex in comparison with the isolated moieties. Refer to Fig. 1 for a definition of the atomic indices. *Dimer* stands for the complex $CH_3CN\cdots H_2O$. Distances in angstroms, angles in degrees, rotational constants in gigahertz and dipole moments in debyes

	MP2/6-311++G(d,p)			MP2/aug-cc-pVDZ			B3LYP/6-311++G(d,p)			B3P86/6-311++G(d,p)		
	CH_3CN	H_2O	Dimer	CH_3CN	H_2O	Dimer	CH_3CN	H_2O	Dimer	CH_3CN	H_2O	Dimer
N1 ≡ C2	1.174		1.172	1.185		1.183	1.153		1.151	1.152		1.151
C2–C3	1.463		1.462	1.471		1.470	1.457		1.455	1.450		1.448
C3–H4(5,6)	1.092		1.091	1.099		1.099	1.092		1.092	1.091		1.091
C2–C3–H4(5)	109.9		109.8	109.9		109.7	110.2		110.0	110.1		110.0
C2–C3–H6	109.9		109.8	109.9		109.8	110.2		110.1	110.2		110.1
N1–H7			2.106			2.060			2.079			2.036
C2–N1–H7			162.9			169.7			167.3			167.4
O8–H7		0.960	0.965		0.966	0.972		0.962	0.968		0.960	0.968
O8–H9		0.960	0.959		0.966	0.965		0.962	0.961		0.960	0.959
H7–O8–H9		103.4	103.0		103.9	103.8		105.1	104.7		104.9	104.5
I_A	158.670		94.248	156.407		105.039	159.158		105.720	159.229		106.323
I_B	9.081		1.742	8.950		1.743	9.245		1.762	9.295		1.795
I_C	9.081		1.729	8.950		1.734	9.245		1.752	9.295		1.785
μ	3.880	2.187	5.853	3.936	1.879	5.773	4.053	2.159	6.147	4.065	2.168	6.202

Similarly, the experimental value [29] of 3.96 D for gaseous CH_3CN is obtained as 3.94 D, in fairly good agreement. All DFT results for the dipole moments of water and CH_3CN are too large. The calculated dipole moment value of 5.77 D for the complex obtained at the MP2/aug-cc-pVDZ level is in good agreement with a previously inferred value of 5.5 D [14]. The present accuracy should be useful in the possible detection of this hydrogen-bonded complex.

Vibrational frequency shifts

The calculated vibrational frequencies for the separate molecules and the hydrogen-bonded complex are shown in Table 2. Acetonitrile has 12 vibrational modes corresponding in fact to eight active fundamentals: four non-degenerate (a_1 symmetry) and four doubly degenerate (*e* symmetry) vibrational frequencies. After complexation the *e*-degenerate modes may split and all vibrational frequencies may shift. The magnitude of the shift may be used for characterization of the structure of the complex. As is well known, after hydrogen binding the symmetric (a_1) and asymmetric (b_2) vibrational frequencies of the water shift to the red, whereas the scissor (a_1) mode in the region of 1,600 cm^{-1} shifts towards the blue. The calculated results are in agreement with this qualitative picture, as seen in Table 2. The redshift of the OH stretching vibration is calculated to vary between –53 and –101 cm^{-1}. The calculated shift at the MP2/aug-cc-pVDZ level is −74 cm^{-1}. For acetonitrile the largest shift is obtained for the intense NC stretching mode. All the theoretical models predict that this shift is toward the blue and that the magnitude varies between 10 and 17 cm^{-1}. This calculated blueshift is in agreement with the decrease in the NC distance, after complexation, obtained theoretically and discussed in the previous section. Stretching vibrations of atoms involved in hydrogen bonds are normally shifted towards smaller vibrational frequencies (redshift). IR blueshifts of stretching modes due to hydrogen bonds are attracting considerable attention after the studies of Hobza and Havlas [32].

Binding energies

The calculated results for the binding energies are shown in Table 3. All the results shown include counterpoise correction to BSSE. Two sets of single-point energy calculations were performed. One is CCSD(T)/6-311++G(d,p) using the geometry obtained previously with the MP2/6-311++G(d,p) method and the other is CCSD(T)/aug-cc-pVDZ using the geometry obtained with the MP2/aug-cc-pVDZ method. Intermediate results, like the incomplete and complete MP4 results, are useful to analyze the electron correlation effects in the binding energy. It can be noted that electron correlation effects are important; they increase the calculated binding energies with respect to the HF result. With the MP2/aug-cc-pVDZ model the binding energy is calculated as 4.45 kcal mol^{-1}. This value is only slightly decreased after including higher-order electron correlation effects. At the highest level, CCSD(T), this value is decreased to 4.23 kcal mol^{-1}. The MP2 results confirm that this is a good theoretical model for calculating binding energies of hydrogen-bonded systems [33, 34]. Of particular importance is the contribution of high-order triple excitation. At the fourth-order the triple excitation contribution, as derived from the difference between MP4 and SDQ-MP4, amounts to +0.25 kcal mol^{-1} in the binding energy. Including all triple excitations derived from the difference between CCSD(T) and CCSD gives a similar result of 0.21 kcal mol^{-1}. Thus, most of the triple excitation contribution to the binding energy is obtained already in fourth order and the total effect of triple excitation is to increase the binding energy by around 5%. Table 3 also shows that single excitations contribute even less to the binding energy. In fourth order, single excitation is

Table 2. Calculated vibrational frequencies of the $CH_3CN\cdots H_2O$ complex and assignment of the calculated frequencies of the monomers. All frequencies in reciprocal centimeters

Vibrational mode	Experimental		MP2/6-311++G(d,p)				MP2/aug-cc-pVDZ				B3P86/6-311++G(d,p)				B3LYP/6-311++G(d,p)			
	Acetonitrile[a]	H_2O[b]	Acetonitrile	H_2O	Dimer	$\Delta\nu$	Acetonitrile	H_2O	Dimer	$\Delta\nu$	Acetonitrile	H_2O	Dimer	$\Delta\nu$	Acetonitrile	H_2O	Dimer	$\Delta\nu$
ν (e)	362		354		356	+2	351		356	+5	384		387	+3	382		385	+3
					360	+6			360	+9			391	+7			389	+7
ν (a_1)	920		933		937	+4	931		936	+5	946		951	+5	929		933	+4
ν (e)	1,042		1,070		1,069	−1	1,048		1,048	0	1,053		1,053	0	1,061		1,061	0
					1,070	0			1,049	+1	–	–	–	–	1,062		1,062	0
ν (a_1)	1,382		1,424		1,424	0	1,391		1,391	0	1,401		1,401	0	1,411		1,411	0
ν (e)	1,448		1,500		1,497	−3	1,467		1,465	−2	1,467		1,464	−3	1,475		1,472	−3
					1,498	−2		–	–				1,465	−2	–	–	–	–
ν (a_1) scissor		1,590		1,630	1,662	+32	–	1,622	1,647	+25		1,603	1,633	+30		1,603	1,632	+29
ν (a_1) NC stretch	2,267		2,211		2,223	+12	2,180		2,197	+17	2,378		2,389	+11	2,363		2,373	+10
ν (a_1)	2,954		3,100		3,101	+1	3,088		3,090	+2	3,062		3,064	+2	3,047		3,049	+2
ν (e)	3,009		3,194		3,197	+3	3,189		3,192	+3	3,142		3,145	+3	3,117		3,121	+4
ν (a_1) symmetric stretch		3,638		3,882	3,829	−53		3,804	3,730	−74		3,853	3,752	−101		3,818	3,739	−79
ν (b_2) asymmetric stretch		3,733		3,999	39,74	−25		3,938	3,906	−32		3,962	3,931	−31		3,923	3,894	−29

[a]From Ref. [30] [b]From Ref. [31]

Table 3. Calculated binding energies (kcal/mol) and electron correlation effects in the hydrogen-bonded complex $CH_3CN\cdots H_2O$. All results were obtained at the optimized MP2 geometries indicated and include counterpoise correction to the basis set superposition error

Method	MP2/6-311++G(d,p)	MP2/aug-cc-pVDZ
HF	3.67	3.23
MP2	4.33	4.45
MP3	4.05	4.08
DQ-MP4	3.97	3.99
SDQ-MP4	4.03	4.08
MP4	4.19	4.33
CCSD	3.99	4.02
CCSD(T)	4.13	4.23

obtained as the difference between the SDQ-MP4 and DQ-MP4 results and contributes only 0.09 kcal mol^{-1} using the aug-cc-pVDZ basis in the MP2/aug-cc-pVDZ optimized geometries, for instance. High-order single excitations are even smaller, as seen using the difference between CCSD and DQ-MP4 results. Again, using the MP2/aug-cc-pVDZ geometry and the aug-cc-pVDZ basis set this is only 0.03 kcal mol^{-1}. This explains why MP2 is a good model for calculating binding energies of hydrogen-bonded systems. Similar results are obtained with the other theoretical models. The results obtained with DFT are slightly larger than those obtained with Møller–Plesset or coupled-cluster theories. The result for the binding energy using exclusively the B3LYP/6-311++G(d,p) method, for both geometry and energies, is 4.81 kcal mol^{-1}. The result of 4.23 kcal mol^{-1} obtained with MP2/aug-cc-pVDZ is in good agreement with the result of 4.18 kcal mol^{-1} obtained in Ref. [14]. Overall, the BSSE amounts to a correction of less than 1.0 kcal mol^{-1} in the binding energy with the correlated models, from MP2 to CCSD(T).

Before giving our best estimate for the binding energy, we should take into account the difference in zero-point vibrational energies. Using the harmonic approximation the calculated frequencies were obtained and are given in Table 2. Using these values we obtained a difference in zero-point vibrational energies of 1.31 kcal mol^{-1}. However, although the intramolecular vibrations may be reasonably well described by the harmonic approximation, the intermolecular vibrations are largely anharmonic. Taking this into consideration, we estimate the difference in zero-point vibrational energies as 0.70 kcal mol^{-1}. Using this result we give our best estimate of the binding energy of the hydrogen-bonded complex as 3.53 kcal mol^{-1}. This result is obtained with the CCSD(T)/aug-cc-pVDZ single-point calculation performed in the MP2/aug-cc-pVDZ geometry and calculated frequencies.

Rayleigh and Raman scattering activities

Light scattering cross-section and depolarization are related to the anisotropy of the electronic polarization of

a molecular system. As the hydrogen-bond formation leads to a change in the anisotropy, it should lead to a corresponding change in the light depolarization. In the case of elastic Rayleigh scattering the degrees of depolarization of the light scattered at right angles to the direction of incidence for natural and plane-polarized light are given by [35, 36, 37, 38]

$$\sigma_n = 6(\Delta\alpha)^2 \Big/ \left[45\alpha^2 + 7(\Delta\alpha)^2\right]$$

and

$$\sigma_p = 3(\Delta\alpha)^2 \Big/ \left[45\alpha^2 + 4(\Delta\alpha)^2\right].$$

The average, α, and anisotropic, $\Delta\alpha$, dipole polarizabilities are the invariants of the polarizability tensor and are obtained from

$$\alpha = \left(\alpha_{xx} + \alpha_{yy} + \alpha_{zz}\right)/3$$

and

$$(\Delta\alpha)^2 = 1/2\left[\left(\alpha_{xx} - \alpha_{yy}\right)^2 + \left(\alpha_{yy} - \alpha_{zz}\right)^2 + \left(\alpha_{zz} - \alpha_{xx}\right)^2\right] + 3\left(\alpha_{xy}^2 + \alpha_{xz}^2 + \alpha_{yz}^2\right).$$

The maximum value [35] of σ in the Rayleigh scattering corresponds to the most anisotropic case, corresponding to the extreme where $\Delta\alpha = 3\alpha$. In this case, $\sigma_n^{max} = 1/2$ and $= 1/3$. It is also of interest to obtain the depolarization for circularly polarized light. The light circularly polarized scattered backwards may have a component of circular polarization. The degree of reversal is given by [35]

$$\sigma_c = \sigma_n/(1 - \sigma_n).$$

It is easy to see that in this Rayleigh case σ_c^{max} is 1.In the inelastic case of the Raman scattering in the same experimental setup the degree of depolarization is given by the same expressions but the derivative with respect to the vibrational mode should be taken. Hence, for the plane-polarized case one has

$$\sigma_p^{(v)} = 3(\Delta\alpha')^2 \Big/ \left[45(\alpha')^2 + 4(\Delta\alpha')^2\right],$$

where the prime indicates a derivative with respect to the v vibrational mode. We calculate the depolarization for all the fundamentals of CH_3CN both isolated and after hydrogen binding with water. In this case the value of σ_p^{max} is 3/4. The cross-section for Raman scattering is completely determined by the scattering activity given by [35]

$$A_p = 45(\alpha')^2 + 7(\Delta\alpha')^2.$$

The change in depolarization is now reported for CH_3CN both isolated and after hydrogen binding with water. The result for the Rayleigh case and also the calculated polarizabilities are given in Table 4. The dipole polarizabilities of both CH_3CN and H_2O are found to be in good agreement with the experimental results. The average dipole polarizability of $CH_3CN\cdots H_2O$, as expected, is only slightly larger than the sum of the dipole polarizabilities of separated CH_3CN and H_2O. The change in the anisotropic polarizabilities of CH_3CN and $CH_3CN\cdots H_2O$ and the increase in the average polarizabilities lead to the variation in the depolarization ratios as given in Table 4. In all cases the depolarization increases upon complexation. The calculated activities for the Raman scattering are given in Table 5. All eight active fundamentals of CH_3CN are considered, but in the case of the degenerate vibrations the depolarization has its maximum value of 3/4 as in this case the derivative of the dipole polarizability evaluated at the origin of the molecular vibration is zero. The largest cross-section for the inelastic scattered light transition is obtained for the CH symmetric mode in the region of 3,090 cm^{-1}; however, for this vibration the depolarization for plane-polarized light is essentially zero and does not change after complexation. In this direction the most important vibrational mode associated with CH_3CN is the NC stretching mode. Its depolarization ratio changes from 0.17 to 0.20 after the hydrogen-bond formation. Another pronounced change in depolarization is obtained for the less intense CC stretching at the calculated frequency of 930 cm^{-1}. In this case the depolarization changes by a percentually large amount of 45%, from 0.07 to 0.10, but the absolute depolarization is smaller than that for the NC stretching and A_p is also smaller. These effects are more pronounced in the H_2O modes. It has been noted before [39] in the water dimer, at the HF level, that the symmetric OH donor vibration increases by nearly 2. The same situation is seen here, where we find a great intensification of the scattering activity for the symmetric stretch vibration of H_2O (Table 5). To make a comparison with the case of the hydrogen-bonded water dimer $(H2O)_2$ we also calculated its scattering activity at the present MP2/aug-cc-pVDZ level. Starting from pure H_2O, the scattering activity of the OH stretching vibration ($104.1a_0^4$/amu) increases by 55% in the water dimer

Table 4. Calculated dipole polarizabilities, both average, α, and anisotropic, $\Delta\alpha$, in atomic units, depolarization ratio for CH_3CN and $CH_3CN\cdots H_2O$. All calculations were made at the MP2/aug-cc-pVDZ level and the corresponding optimized geometries

Molecule	α[a]	$\Delta\alpha$	σ_n	σ_p	σ_c
H_2O	9.30	1.04	0.0017	0.0008	0.0017
CH_3CN	29.43	15.65	0.0361	0.0184	0.0375
$CH_3CN\cdots H_2O$	39.67	21.78	0.0384	0.0196	0.0399

[a]Experimental value [27] for the dipole polarizability of water is 9.80 au and for acetonitrile two values are reported, 29.72 and 30.27 au

Table 5. Calculated Raman activities A_p (a_0^4/amu) and depolarization of plane-polarized light for CH_3CN and $CH_3CN\cdots H_2O$. All calculations were made at the MP2/aug-cc-pVDZ level and the corresponding optimized geometries

Vibrational mode	CH_3CN		H_2O		$CH_3CN\cdots H_2O$	
	A_p	σ_p	A_p	σ_p	A_p	σ_p
ν ($1a_1$)	7.07	0.071	–	–	7.92	0.101
ν ($2a_1$)	3.48	0.432	–	–	3.90	0.418
ν ($3a_1$) NC stretch	49.37	0.169	–	–	64.02	0.202
ν ($4a_1$)	188.21	0.002	–	–	196.37	0.005
ν ($1a_1$)scissor	–	–	1.95	0.633	0.58	0.644
ν ($2a_1$)symmetric stretch	–	–	104.10	0.042	206.78	0.153
ν ($1b_2$)asymmetric stretch	–	–	24.17	0.750	40.94	0.484

$H_2O\cdots H_2O$ ($161.6a_0^4$/amu) and increases by 99% ($206.8a_0^4$/amu) in the case of $CH_3CN\cdots H_2O$. This is indicative of a stronger bond and corroborates the result for the frequency shift of -74 cm^{-1} calculated for the symmetric OH stretch in the vibrational spectrum. As to the depolarization ratio, we may note that it changes from a factor of nearly 4 from the free water (0.042) to the $CH_3CN\cdots H_2O$ complex (0.153).

Summary and conclusions

The hydrogen-bond interaction between acetonitrile and water, CH3CN$\cdots$H$_2$O, has been analyzed by ab initio methods. Geometry optimization, vibrational frequencies, Rayleigh and Raman activities including light scattering depolarization and binding energies were considered. The geometries of the complex and of the separate moieties were calculated using different theoretical models. In all the models we found a shortening of the NC distance, leading to a blueshift of around 15 cm^{-1} in the IR spectrum. The calculated hydrogen-bond N–H distance at the MP2/aug-cc-pVDZ level is 2.06 Å, with small variations between the results obtained using the different theoretical methods. The dipole moment of the complex $CH_3CN\cdots H_2O$ is 5.77 D in good agreement with the suggestion of Desfrançois et al. [14]. The binding energy was obtained using different theoretical models and the role of electron correlation effects was analyzed. Taking into account the BSSE and the difference in zero-point anharmonic vibrational energies our best estimate for the binding energy is 3.53 kcal mol^{-1}, obtained with the CCSD(T)/aug-cc-pVDZ single-point calculation performed in the MP2/aug-cc-pVDZ geometry and calculated frequencies. Of particular interest here are the Rayleigh and Raman cross-section depolarization ratios. A light scattering analysis was made both for the elastic Rayleigh and for the inelastic Raman cases after calculation of the dipole polarizabilities and their corresponding derivatives with respect to the intramolecular vibrational modes, at the MP2/aug-cc-pVDZ level. The calculated average dipole polarizability is 39.67 au and the anisotropy is fairly large, corresponding to 21.78 au. The depolarization of the light scattered was then reported for the $CH_3CN\cdots H_2O$ complex and the results were compared with the results obtained for the two separated moieties. It is noted that in the Raman case the depolarization due to the intense NC stretching vibration is increased by 20%. For the OH symmetric stretch of water there is a large redshift of 75 cm^{-1} in the vibrational frequency and a great intensification of the Raman scattering activity: the cross-section increases by a factor of 2 and the depolarization by a factor of nearly 4.

Acknowledgements. This work was partially supported by CNPq and FAPESP (Brazil).

References

1. Shin DN, Wijnen JW, Engberts JBFN, Wakisaka A (2002) J Phys Chem B 106:6014
2. Engberts JBFN, Blandamer MJ (2002) J Chem Commun 18:1701
3. Plašil R, Glosik J, Zakouřil P (1999) J Phys B At Mol Opt Phys 32:3575
4. Pratap P, Megeath ST, Bergin EA (1999) Astrophys J 517:799
5. Kalenskii SV, Promislov VG, Alakoz AV, Winnberg A, Johansson LEB (2000) Astron Astrophys 354:1036
6. Kalenskii SV, Promislov VG, Alakoz AV, Winnberg A, Johansson LEB (2000) Astron Rep 44:725
7. Kim HD, Cho SH, Chung HS, Kim HR, Roh DG, Kim HG, Minh YC, Minn YK (2000) Astrophys J Suppl Ser 131:483
8. Scoles G (ed) (1990) The chemical physics of atomic and molecular clusters. North-Holland, Amsterdam
9. Bernstein ER (ed) (1990) Atomic and molecular clusters. Elsevier, Amsterdam
10. Buckingham AD, Fowler PW, Hutson JM (1988) Chem Rev 88:963
11. Scheiner S (1997) Hydrogen bonding: a theoretical perspective. Oxford University Press, Oxford
12. Zwier TS (1996) Annu Rev Phys Chem 47:205
13. Caminati W, Moreschini P, Favero PG (1998) J Phys Chem A 102:8097
14. Desfrançois C, Abdoul-Carime H, Khelifa N, Schermann JP, Brenner V, Millie P (1995) J Chem Phys 102:4952
15. Desfrançois C, Abdoul-Carime H, Schulz CP, Schermann JP (1995) Science 269:1707
16. Smith DA (ed) (1994) Modeling the hydrogen bond. ACS symposium series 569. American Chemical Society, Washington, DC
17. Malaspina T, Coutinho K, Canuto S (2002) J Chem Phys 117:1692
18. Damewood JR, Kumpf RA (1987) J Phys Chem 91:3449
19. Burneau A, Schriver L, Manceron L, Perchard JP (1985) J Chim Phys PCB 82:19
20. Lee C, Yang W, Parr RG (1988) Phys Rev B 37:785
21. Becke AD (1988) Phys Rev A 38:3098
22. Perdew JP (1986) Phys Rev B 33:8822
23. Wilson A, van Mourik T, Dunning TH Jr (1996) J Mol Struct (THEOCHEM) 388:339
24. Raghavachari K (1991) Annu Rev Phys Chem 42:615
25. Boys SF, Bernardi F (1970) Mol Phys 19:553

26. Frisch MJ, Trucks GW, Schlegel HB, Scuseria GE, Robb MA, Cheeseman JR, Zakrzewski VG, Montgomery JA Jr, Stratmann RE, Burant JC, Dapprich S, Millam JM, Daniels AD, Kudin KN, Strain MC, Farkas O, Tomasi J, Barone V, Cossi M, Cammi R, Mennucci B, Pomelli C, Adamo C, Clifford S, Ochterski J, Petersson GA, Ayala PY, Cui Q, Morokuma K, Malick DK, Rabuck AD, Raghavachari K, Foresman JB, Cioslowski J, Ortiz JV, Baboul AG, Stefanov BB, Liu G, Liashenko A, Piskorz P, Komaromi I, Gomperts R, Martin RL, Fox DJ, Keith T, Al-Laham MA, Peng CY, Nanayakkara A, Gonzalez C, Challacombe M, Gill PMW, Johnson B, Chen W, Wong MW, Andres JL, Gonzalez C, Head-Gordon M, Replogle ES, Pople JA (1998) Gaussian 98, revision A.7. Gaussian, Pittsburgh, PA
27. Lide DR (ed) (1992) Handbook of chemistry and physics, 73rd edn, CRC, Boca Raton, FL
28. Lovas FJ (1978) J Phys Chem Ref Data 7:1445
29. Christophorou LG, Christodoulides AA (1969) J Phys B At Mol Opt Phys 2:71
30. Koga Y, Kondo S, Saeki S, Person WB (1984) J Phys Chem 88:3152
31. Bentwood RM, Barnes A, Orville-Thomas W (1980) J Mol Spectrosc 84:391
32. Hobza P, Havlas Z (2000) Chem Rev 100:4253
33. Rivelino R, Canuto S (2000) Chem Phys Lett 322:207
34. Scheiner S, Kar T, Gu Y (2001) J Biol Chem 276:9832
35. Herzberg G (1945) Infrared and Raman spectra of polyatomic molecules. Van Nostrand, Princeton, NJ
36. Suzuki H (1979) Prog Theor Phys 62:936
37. Castro MA, Canuto S (1993) J Phys B 26:4301
38. Serrano A, Canuto S, Castro M (1999) J Mol Struct (THEOCHEM) 489:29
39. Swanton DJ, Bacskay GB, Hush NS (1984) Chem Phys 83:69